Est. 1984

ORIENTAL JOURNAL OF CHEMISTRY
An International Open Access, Peer Reviewed Research Journal

www.orientjchem.org

ISSN: 0970-020 X
CODEN: OJCHEG
2023, Vol. 39, No.(1):
Pg. 01-10

Drug Repurposing against Phosphomannomutase for the Treatment of Cutaneous Leishmaniasis

SABAHAT YASMEEN SHEIKH[1], WASEEM AHMAD ANSARI[2], FIROJ HASSAN[1], MOHAMMAD FAHEEM KHAN[2], SYED SHAH MOHAMMED FAIYAZ[4], YUSUF AKHTER[3], ABDUL RAHMAN KHAN[1] and MALIK NASIBULLAH[1]*

[1]Department of Chemistry, Integral University, Dasauli, Kursi Road, Lucknow-226026 India.
[2]Department of Biotechnology, Era University, Sarfarazganj, Hardoi Road, Lucknow-226003 India.
[3]Department of Biotechnology, Babasaheb Bhimrao Ambedkar University, VidyaVihar, Raebareli Road, Lucknow-2260025 India.
[4]Department of Physiology, College of Medicine, Hail University-81442, Saudi Arabia.
*Corresponding author E-mail: malik@iul.ac.in

http://dx.doi.org/10.13005/ojc/390101

(Received: November 07, 2022; Accepted: January 10, 2023)

ABSTRACT

Due to the lack of approved vaccines against Cutaneous leishmaniasis (CL), chemotherapy is the only treatment option. Presently, none of the current CL drugs have high levels of efficacy and safety profiles. Thus, the development of new and safer drugs is urgently needed. Drug repurposing can be used for the development of new therapeutic activities. Phosphomannomutase (PMM) has become highlighted as a potential drug target due to its important role in the biosynthesis of glycoconjugates which is essential for parasite virulence. To identify new promising lead molecules, we have performed virtual screening of 8,500 drugs and selected 46 drugs for docking simulation through the Glide module of Schrodinger software. The saquinavir and grazoprevir showed the highest binding affinity (-10.144 and -10.131 kcal/mole). To find the stability of both complexes, molecular dynamics (MD) simulations were performed at 100ns. The grazoprevir-2i54 and saquinavir-2i54 complexes showed good stability in the active site of the receptor. It could be an alternative drug for the treatment of CL.

Keywords: Drug Repurposing, Phosphomannomutase, Molecular Docking Simulations, Molecular Dynamics Simulation, Amphotericin B, Miltefosine.

INTRODUCTION

Leishmaniasis is caused by the protozoan parasite of the 20 Leishmania species and disseminated through the bite of female phlebotomine sandfly species.[1,2] During its life cycle, the parasite switches from a promastigote flagellate form within the sandfly to an intracellular amastigote form in the macrophages of the mammalian host.[3] It is included among 13 neglected tropical parasitic diseases by the World Health Organization Tropical Disease Research

(WHO TDR).[4] The disease mainly attacks the poor and is associated with malnutrition, population displacement, poor housing, and a weak immune system. This disease is recognized in the three most variable forms, such as Cutaneous leishmaniasis, Mucocutaneous leishmaniasis, and Visceral leishmaniasis. Cutaneous leishmaniasis is the most common form, recognized as skin scratches, stigma, ulcers, and scars. This disease is mostly distributed in America, the Mediterranean Basin, the Central and Middle East Asia. In September 2021, CL occurred in 56 endemic countries reported by the WHO Global Leishmaniasis program for 2020. In 2020, about 80% of global CL was reported from 7 countries (Afghanistan, Algeria, Colombia, Iraq, Pakistan, Seria, and the Arab Republic). It is estimated that 6,00,000 to 1 million new cases are reported worldwide annually.[5] There are two important ways to affect the development of the parasite within the host, considering proteins expressed in the amastigote form as therapeutic targets. The first one targeting proteins in biochemical pathways is leading to altered metabolism and is harmful to the parasite.[6-9] Another one is to avoid macrophage-parasite which plays a pivotal role in glycoconjugate recognition. Inhibition of glycoconjugate biosynthesis diminishes parasite load. Glycosylation is a key pathway for macrophage infection.[10-14] PMM is a chief therapeutic target that plays an essential role in the survival of the parasite in the mammalian life cycle.[15] It converts mannose-6-phosphate to mannose-1-phosphate which is an essential step in mannose activation and the biosynthesis of glycoconjugates such as Glycosylphosphatidylinositol (GPI), Lipophsophoglycan (LGP), Proteophosphoglycans (PPG), and Glycoinositolphospholipid (GIPLS) which are present at the surface of the eukaryotic cell and involved in many biological processes like intercellular recognition, adhesion or signaling.[16,17] These glycoconjugates are essential for parasite virulence.[11,14] Removal of PMM from *Leishmania mexicana* results in the loss of virulence which recommended that PMM is a promising drug target for the development of anti-leishmanial inhibitors.[18] Pentavalent antimonials have been used for decades against CL, but due to adverse side effects like musculoskeletal pain, gastrointestinal disturbances, and mild to moderate headaches cannot be used frequently. The current treatment options are liposomal amphotericin B, miltefosine, fluconazole, and ketoconazole.[19] These treatments have serious issues including prolonged treatment, parenteral administration, tolerability, teratogenicity, etc.[20] Nowadays, none of the current CL drugs have high levels of efficacy, safety and short duration of treatment. Thus, the development of new and safer drugs having cost-effective, efficacious, oral, and short-course drugs for CL is urgently needed. Drug repurposing is an alternative method for the development of new drugs. Approved drugs have known pharmacokinetics and safety profiles.[21,22] When a new biological activity has been identified, the drug can be rapidly advanced into clinical trials. Here, we have selected 8500 approved drugs for their potential to be repurposed for CL.

METHODS

Target preparation and validation

For the preparation of receptors for docking, the 3D structures of PMM (PDB-ID:2i54) were retrieved from Protein Data Bank (http://www.rcsb.org/pdb) in PDB format with resolution value 2.10 Å & R-values; free 0.230 and work 0.189. The crystal structure of PMM has three chains A, B, and C. The receptor was prefabricated by using protein preparation wizard Maestro module 2.6.144 Schrodinger 2020-4 LCC, New York USA software. At the initial step removed the heteroatoms, and water molecules from the receptor. Further, it was preprocessed by adding missing hydrogen atoms, assigning the bond order, creating zero-bond order to metals, disulfide bonds, and converting the selenomethionines to methionines with generating heteroatoms states at 7.0+/-2.0 Epik pH. Now finally, the receptor was optimized with the help of PROPKA 7.0 pH and then performed restrained minimization by applying OPLSe force field. Furthermore, the binding pocket of the receptor was elucidated by selecting a native ligand (citric acid) for the grid generation and the grid box was positioned over the binding pocket of the receptor.[23] It represents that protein structure is best for docking analysis.[24]

Prochek Ramachandran plot was used for the validation of target protein (2i54) defined by the phi (φ) and psi (ψ) angles, the number of amino acid residues shown in the most favorable region is 90.8%, the additional allowed region is 8.9%, generously allowed regions are 0.3% and

disallowed region is 0.0%. The number of amino acid residues was shown >90% which represents good quality of 3D model[25]. After the validation of the protein, docking analysis was performed to find out the protein-ligand interaction.[26]

Procheck statistics

	No. of residue	%age
Most favoured regions [A,B,L]	583	90.8%
Additional allowed regions [a,b,l,p]	57	8.9%
Generously allowed regions [~a,~b,~l,~p]	2	0.3%
Disallowed regions[XX]	0	0.0%
Non-glycine and non-proline residues	642	100.0%
End-residues (excl. Gly and Pro)	6	
Glycine residues	57	
Proline residues	21	
Total number of residues	726	

Ligand preparation

We have retrieved 8500 drugs from the Zinc database and saved in PDB format after being explored in the discovery studio visualization tool. [27] Open Babel was used for the energy minimization of ligands[28] and converted into pdbqt format with the help of a PyRx virtual screening tool for the protein-ligand interaction analysis.[29] For revalidating, the docking score of lead compounds again performed the molecular docking through the Maestro module 12.6.144 Schrodinger 2020-4 LCC, New York USA software. So, the chosen compounds have been drawn by a 2D sketcher and saved in the project table. The 2D structures were converted into 3D structures by correcting the geometry and generating the conformers. All the structures were optimized by adding missing hydrogen atoms. They stirred-up all the ligands with possible states between the Epik pH 7.0+/-2.0. Finally, the OPLSe force field was applied on all ligands and minimized by using the LigPrep module of Maestro12.6.144 Schrodinger 2020-4 LCC.

Virtual Screening and molecular docking

The virtual screening of 8500 drugs was carried out by AutoDock Vina PyRx 0.8 against PMM (PDB ID: 2i54) and energy was minimized through open Babel PyRx 0.8 to get the stable and low energy conformation of the protein. AutoDock Vina version PyRx 0.8 tool was used for high-throughput screening of ligands on macromolecular protein (grid box i.e., xyz center value; x:36.69, y:6.52, z:40.38 and dimensions in x:57.36, y:52.56, and z:54.89. The analysis of docking is based on the Lamarckian Genetic Algorithm.[30] After each protein-ligand complex interactions, among the 9 poses, the best pose based on its conformation and binding affinity was selected, and obtained RMSD (Root Mean Square Deviation) values.[31] The RMSD values (UB/LB) zero refers to good interaction between protein and ligand. I have selected the top 46 ligands based on high binding energy. Furthermore, the flexible molecular docking has been validated by redocking the method of standard precision (SP) by using Glide v8.8 Schrodinger 2020-4 LCC. The Van der Waals radii scale was 0.80 along with the partial charge cutoff at 0.15. All the ligands were docked in the binding pocket of the intended receptor and the best pose was selected based on the binding energy, hydrophobic interactions, hydrogen bonds, internal energy, root mean square deviation, and desolvation.

Molecular dynamics simulation

The MD simulation were carried out using Desmond module version 12.6.144 Schrodinger 2020-4 LLC for the top two lead drug molecules, saquinavir (ZINC26664090) and grazoprevir (ZINC95551509). Both complexes were prepared by using a system builder module by applying the OPLSe force field to the TIP3P model of water molecules and setting up the orthorhombic periodic boundary as well as adding Na^+/Cl^- ions to neutralize complexes. The MD simulation were performed at 100ns under condition 300K temperature with 1 bar pressure along with the isobaric NPT equilibrium using the Nose-Hoover thermostat method and trajectory was recorded energy for each 1.2 ps interval. The resulting 100ns MD simulations analyzed root mean square deviation (RMSD) and root mean square fluctuation RMSF of protein and ligand interactions.[32]

RESULTS

Virtual screening and binding interaction analysis

The top 2 lead molecules (saquinavir and grazoprevir) were selected based on the best binding interaction with the 2i54 receptor. The lead compounds saquinavir, and grazoprevir showed excellent binding energy -10.144, -10.131 kcal/mole compared to control drugs Amphotericin B and Miltefosine -7.485 Kcal/mole, -5.734 Kcal/mole respectively Table 1.

Table 1: Molecular docking simulation

S. No	Compound name/Zinc Id	PyRx Binding Energy	Schrodinger Docking Score	Glide gscore	Glide emodel	Common uses
1	Saquinavir ZINC26664090	-8.9	-10.144	-10.158	-120.006	HIV/AIDS
2	Grazoprevir ZINC95551509	-8.5	-10.131	-10.137	-120.225	Hepatitis C
3	Glecaprevir ZINC164528615	-9.0	-9.755	-9.758	-120.135	hepatitis C
4	Olysio ZINC164760756	-8.6	-9.704	-9.71	-96.478	Hepatitis C
5	Methyltetrahydrofolate ZINC2005305	-8.0	-9.425	-9.441	-104.453	Anemia
6	Isavuconazonium ZINC49637509	-8.1	-8.868	-9.372	-117.313	Fungal infections
7	Ceftarolinefosamil anhydrous base ZINC96006023	-8.0	-8.841	-9.143	-134.132	Antibiotic
8	Valstar ZINC28232750	-8.7	-8.809	-8.81	-100.86	High blood pressure and heart failure
9	Capastat ZINC150338698	-8.3	-8.761	-9.273	-109.597	Tuberculosis (TB)
10	Bromocriptine ZINC53683151	-8.6	-8.66	-8.839	-92.616	Parkinson's disease
11	Naldemedine ZINC100378061	-9.0	-8.545	-8.938	-97.355	Constipation
12	Accolate ZINC896717	-8.4	-8.499	-8.506	-108.308	Asthma
13	Sqv ZINC26985532	-9.1	-8.483	-8.496	-102.175	HIV
14	Edoxaban ZINC43200832	-8.2	-8.335	-8.566	-90.036	Strokes or blood clots
15	Brigatinib ZINC148723177	-8.5	-8.283	-8.296	-87.1	lung cancer
16	Olaparib ZINC40430143	-8.1	-7.97	-7.97	-79.842	Cancer
17	Demeclocycline ZINC100036924	-8.0	-7.858	-8.054	-70.308	Bacterial infections respiratory tract infections, infections of the skin
18	Maraviroc ZINC100003902	-8.2	-7.723	-7.723	-78.609	Human immunodeficiency virus (HIV)
19	Emend ZINC27428713	-8.6	-7.451	-7.451	-69.365	Nausea and vomiting
20	Daclatasvir ZINC68204830	-8.6	-7.355	-8.608	-95.033	Chronic-hepatitis C, infection of the liver
21	Doxazosin ZINC94566092	-8.0	-7.208	-7.338	-64.468	High blood pressure
22	Amaryl ZINC537791	-8.0	-7.087	-7.11	-86.168	Diabetes high blood sugar
23	Glimepirid ZINC100070954	-8.7	-7.084	-7.108	-85.984	Type 2 diabetes mellitus (T2DM) to improve glycemic control
24	Flibanserin ZINC52716421	-8.2	-7.064	-7.075	-60.438	HSDD
25	Noxafil ZINC28639340	-8.0	-6.943	-6.961	-72.33	Hematopoietic stem cell transplant
26	Cabozantinib ZINC70466416	-8.2	-6.797	-8.347	-94.422	Cancer, hepatocellular carcinoma liver cancer
27	Tipranavir ZINC100016058	-8.0	-6.711	-6.849	-75.598	Acquired immunodeficiency syndrome (AIDS)
28	Aptivus ZINC100022637	-8.5	-6.706	-6.844	-75.575	HIV/AIDS
29	Abemaciclib ZINC72318121	-8.0	-6.667	-7.485	-83.038	Breast cancer
30	Sorafenib ZINC1493878	-8.1	-6.647	-6.659	-67.537	Kidney, liver, and thyroid cancer
31	Cobimetinib ZINC60325170	-8.3	-6.414	-6.416	-60.058	Skin cancer (melanoma)
32	Lumacaftor ZINC64033452	-8.3	-6.413	-6.413	-79.4	Reduce the risk of lung infections
33	Suvorexant ZINC49036447	-8.9	-6.28	-6.28	-60.096	Insomnia
34	Zelboraf ZINC52509366	-8.0	-6.11	-6.489	-68.725	Skin cancer
35	Dabrafenib ZINC68153186	-8.2	-6.041	-6.457	-61.879	Skin cancer
36	Nebivolol ZINC607986	-8.1	-5.819	-7.843	-83.448	Beta blocker, high blood pressure and heart failure
37	Lapatinib ZINC1550477	-8.2	-5.23	-6.398	-82.687	Breast cancer
38	Lifitegrast ZINC84668739	-8.3	-5.097	-5.097	-75.912	Dry eye disease
39	Ergotamine ZINC52955754	-9.3	-5.087	-7.426	-85.025	Migraine headaches
40	Lomitapide ZINC27990463	-9.5	-4.984	-4.987	-54.714	Familial hypercholesterolemia
41	Niraparib ZINC43206370	-8.0	-4.935	-4.935	-51.749	Peritoneal cancer
42	Azelastine ZINC897240-8.1	-4.199	-4.2	-49.306		Allergy symptoms
43	Visudyne ZINC150338699	-8.0	-4.165	-4.166	-60.702	Eye conditions
44	Telotristat ZINC84758235	-8.1	-4.141	-4.167	-62.629	Diarrhea caused by carcinoid tumors
45	Ceritinib ZINC96272772	-8.1	-3.78	-3.78	-57.205	Non-small cell lung cancer
46	Irinotecan ZINC1612996	-8.7	-3.026	-3.028	-50.8	Cancer
47	Amphotericin B	-9.3	-6.199	-7.485	-83.038	Anti- leishmanial
48	Miltefosine	-5.5	-5.734	-5.734	-59.354	Anti- leishmanial

The amino acids of the active site of the receptor were docked with saquinavir into the binding pocket and exhibited binding interactions such as Van der Waals, salt bridge, conventional hydrogen bond, carbon-hydrogen bond, metal acceptor, pi-anion, pi-alkyl with ASP187, ASN70, PHE11, GLY53, GLY54, VAL11, GLY212, VAL173, GLY174, GLY175, LYS208, ARG122, MET125, SER172, ASN214, ASP12, GLY45, ASP10, MRG2002, ASP180, ARG19, LYS50. Out of these interactions, the ligand indicated five hydrogen bond interactions (one hydrogen bond with ASP 12, ASN214, and three with ASP180 along with one ionic bond). Similarly, the amino acids of the active site involved in the binding interaction of grazoprevir showed interactive forces such as Van der Waals, attractive charge, conventional hydrogen bond, carbon-hydrogen bond, metal acceptor, unfavorable acceptor-acceptor, pi-carbon, pi-alkyl with SER46, GLY174, ASP12, GLY44, PRO18, LYS188, ARG19, ASP207, VAL173, GLY213, GLY175, TRY216, GLU217, PHE182, ASP187, ASN70, MET125, MG2002, ASP180, ASN214, LYS208, SER172, ASP10, MG2002, ASP180, ARG112. Out of these interactions, grazoprevir was bounded with GLY212, and ASN214 along with two hydrogen bonds as well as formed one pi-pi interaction with ARG122. Fig. 1 Furthermore, both complexes were built for molecular dynamic simulations Table 2.

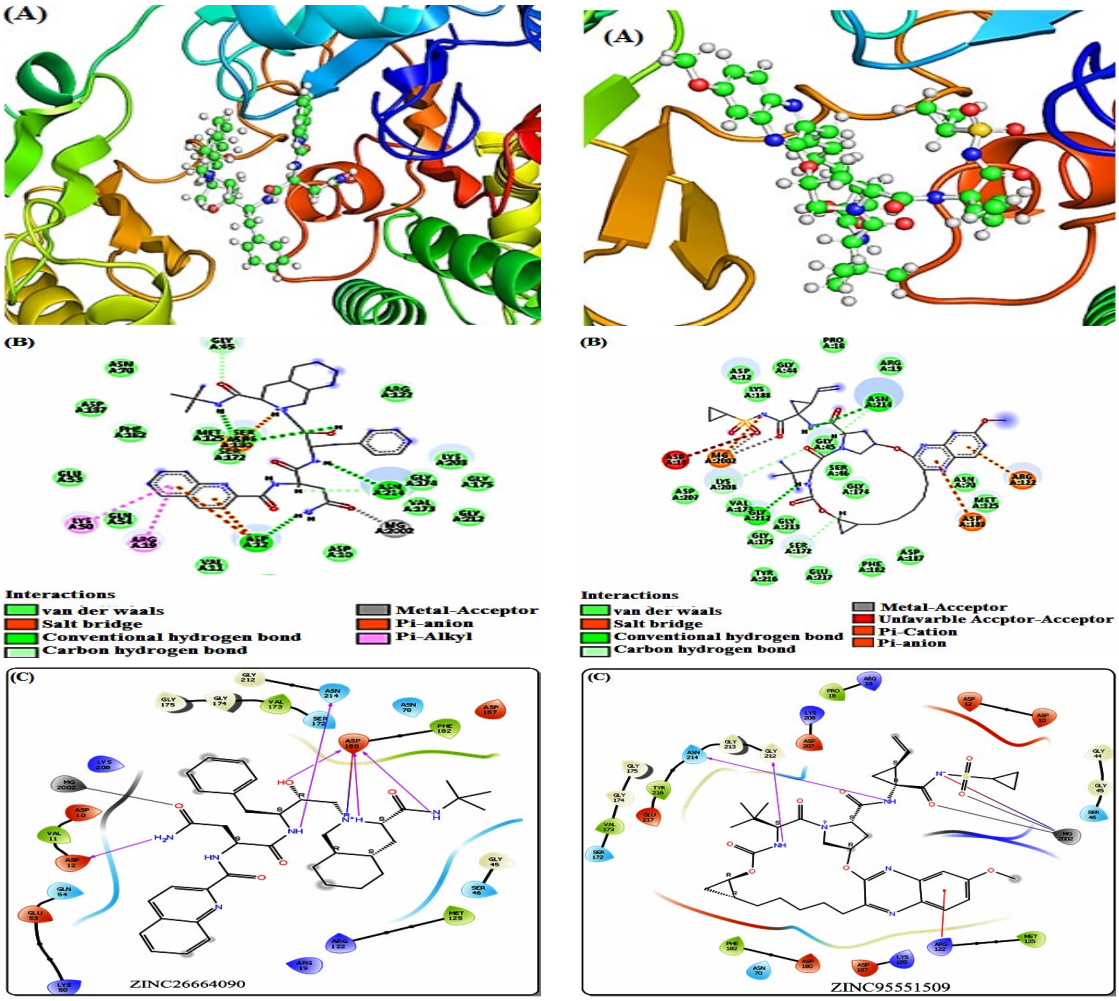

A: 3D Complex structure of ZINC26664090 (Saquinavir) with protein Phosphomannomutase (PDB ID: 2i54) shown docking poses, B: Applied interaction forces in protein and ligand, C: 2D structure of ZINC26664090 with protein Structure (PDB ID: 2i54)

A:3D Complex structure of ZINC95551509 (Grazoprevir) with protein Structure (PDB ID: 2i54) shown docking poses, B: Applied interaction forces in protein and ligand, C: 2D structure of ZINC95551509 with protein Structure (PDB ID: 2i54)

Fig. 1. Interaction details of ZINC26664090 (Saquinavir) and ZINC95551509 (Grazoprevir) through 3D and 2D structure

Table 2: Interaction information from docking calculations between saquinavir and grazoprevir with PMM

Comp. Name/Zinc ID	Interacting amino acids	Applied forces
Saquinavir/ZINC26664090	ASP187, ASN70, PHE11, GLY53, GLY54, VAL11, GLY212, VAL173, GLY174, GLY175, LYS208, ARG122, MET125, SER172, ASN214, ASP12, GLY45, ASP10, MRG2002, ASP180, ARG19, LYS50	• Van Der Waals • Salt bridge • Conventional hydrogen bond • Carbon hydrogen bond • Metal acceptor • Pi-anion • Pi alkyl
Grazoprevir/ZINC95551509	SER46, GLY174, ASP12, GLY44.PRO18, LYS188, ARG19, ASP207, VAL173, GLY213, GLY175, TRY216, GLU217, PHE182, ASP187, ASN70, MET125, MG2002, ASP180, ASN214, LYS208, SER172, ASP10, MG2002, ASP180, ARG112	• Van Der Waals • Attractive charge • Conventional hydrogen bond • Carbon hydrogen bond • Metal acceptor • Un favorable acceptor-acceptor • Pi-cation • Pi alkyl

Molecular dynamics simulation studies

MD simulation are used to optimize and establish the stability of the protein-ligand complex. This study was performed by computing through RMSD and RMSF, analysis of Cα, ligand properties, the radius of gyration (Gy), molecular surface area (MSA), solvent accessible surface area (SASA), polar surface area (PSA), hydrophobic bonds, ionic bonds and water bridges. The highest binding affinity of saquinavir-2i54 & grazoprevir-2i54 complexes were selected for MD simulation studies. We have performed MD simulation of an open dimer of the PMM protein-ligand complex. PMM interchanges the mannose-6-phosphate to mannose-1-phosphate, and glucose 1,6-bisphosphate demonstrated a cofactor for the enzymatic activity of PMM. Thus, the enzyme transfers a phosphate to the aspartyl nucleophile and produces aspartyl phosphate that reorients the enzyme and gets unsettled stability.

Estimation of complex stability via RMSD analysis

During MD simulation studies, RMSD is one of the most important parameters which give complete information about the stability and insight into the structural conformation of the protein-ligand complex. The lower range of RMSD along with consistent variation throughout the simulation showed maximum stability of the protein-ligand complex. In the molecular dynamics simulation of the saquinavir-2i54 & grazoprevir-2i54 complex, structural variations of Cα atoms have first been individually determined for each point during the RMSD analysis.

To calculate the RMSD value of the saquinavir-PMM complex from start to end of the simulation the RMSD of Cα and saquinavir varied from 0.979-4.937 Å and 1.582-4.935 Å [Fig. 2A]. Saquinavir was shown to be stable and bound with protein throughout the simulation. But the protein deviated from the stage of 2.10 to 4.11ns and again achieved the equilibrium point at the end of the simulation. Similarly, the grazoprevir-2i54 complex also computed the RMSD of protein and ligands 1.075-3.663 Å and 1.935-5.655 Å [Fig. 2B]. From the initial to 55ns grazoprevir bound in the active site with rotational movements with the conformational changes but for some times 55.80 to 58.70ns exhibited translational movement with the protein and again attained the equilibrium with the rotational movements in the binding pocket of the protein. After analyzing the RMSD values of both complexes which demonstrated good stability against the target protein Table 3.

Estimation of complex stability via RMSF analysis

RMSF measures the fluctuation in atoms of protein with the ligand during the MD simulation at a specific temperature and pressure. The RMSF values were analyzed at 0.690-5.526 Å and 0.498-5.655 Å for saquinavir-2i54 and grazoprevir-2i54 complexes respectively. Most of the fluctuations were noted in the loop region in which Glu22, Gly212, and Asp245 amino acids of chain B with their RMSF 4.61 Å, 5.08 Å, and 5.526 Å in the saquinavir-2i54 complex [Fig. 3C]. Similarly, the fluctuations were examined in Arg19, and Pro112 with their RMSF 2.00 Å, 2.55 Å, and 3.83Å in the grazoprevir-2i54 complex [Figure 2D].

The grazoprevir-2i54 complex analyzed few positional changes than saquinavir-2i54 during the 100ns MD simulation Table 3.

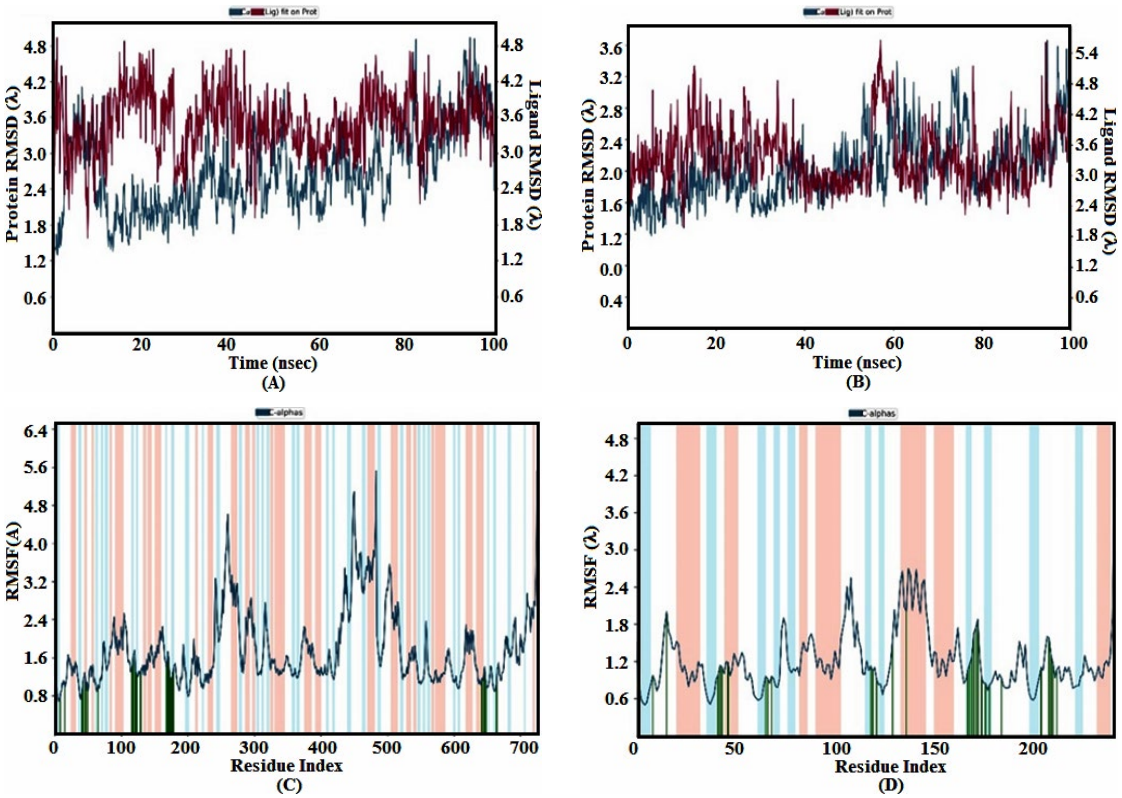

Fig. 2. (A-B) RMSD graph of Saquinavir-2i54 and Grazoprevir-2i54 complex. (C-D) RMSF graph of saquinavir -2i54 and grazoprevir-2i54 complex during 100 ns molecular dynamics simulation

Table 3: Molecular dynamics simulation studies of two lead molecules

Parameters	2i54-Saquinavir	2i54-Grazoprevir
RMSD C atoms (Å)	0.979-4.937	1.075-3.663
RMSD ligand fit on protein (Å)	1.582-4.935	1.935-5.655
RMSF C atoms (Å)	0.690-5.526	0.498-3.835
rGyr (Å)	4.973-5.626	5.148-5.930
MolSA (Å^2)	548.929-619.015	602.875-674.166
SASA (Å^2)	171.793-372.838	316.886-669.971
PSA (Å^2)	135.771-214.001	159.518-223.044
Hydrogen bonds	A: Arg19, A: Ser46, A: Asn127, A: Arg133, A: Gly174, A: Gln176, A: Ser178, Asp180, C: Pro165, C: Asp166, C: Gln168	A: Arg19, A: Lys50, A: Asn70, A: Arg122, A: Ser172, A: Val 173, A: Gly175, A: Gln176, A: Lys188, A: Gly212, A: Gly213, A: Asn214
Hydrophobic bonds	A: Arg122, A: Met125, A: Arg133, A: Ile177, A: Phe182 C: Lys184	A: Leu72, A: Arg122, A: Met125, A: Val173, A: Phe182, A: Lys188, A: Tyr216
Ionic bonds	A: Asp180	A: Asp12, A: Arg19, A: Lys50
Water bridges	A: Arg19, A: Gly45, A: Ser46, A: Lys50, A: Arg122, A: Asn127, A: Arg133, A: Ser172, A: Val173, A: Gly174, A: Gly175, A: Gln176, A: Ile177, A: Ser178, A: Asp180, C: Pro165, Asp166, C: Gln168	A: Asp12, A: Arg19, A: Gly45, A: Ser46, A: Asp47, A: Lys50, A: Glu69, A: Asn70, A: Arg122, A: Asn123, A: Arg133, A: Arg140, A: Tyr171, A: Ser172, A: Val173, A: Gly174, A: Gly175, A: Gln176, A: Asp180, A: Lys188, A: Lys208, A: Gly212, A: Gly213, A: Asn214

RMSD C=Root mean square deviation of Protein, RMSD ligand=Root mean square deviation of ligand, RMSF C=Root mean square fluctuation of protein, rGyr=Radius of Gyration, MolSA=Molecular Surface Area, SASA=Solvent Accessible Surface Area, PSA=Polar Surface Area

Analysis of protein-ligand interaction and ligand properties

To calculate protein-ligand interactions, based on molecular docking results, the complexes which displayed the lowest binding energies against the receptor were chosen. To check the stability of respective complexes performed MD simulation at 100ns in which hydrogen bond, hydrophobic interaction, ionic bond, and water bridges were explored. As a result total of eleven hydrogen bonds (A: Arg19, A: Ser46, A: Asn127, A: Arg133, A: Gly174, A: Gln176, A: Ser178, Asp180, C: Pro165, C: Asp166, and C: Gln168), out of these amino acids Asp180 involved 99% to form a hydrogen bond with saquinavir, six hydrophobic interactions (A: Arg122, A: Met125, A: Arg133, A: Ile177, A: Phe182 C: Lys184) with interacting amino acids, one ionic bond (A: Asp180) and eighteen water bridges (A: Arg19, A: Gly45, A: Ser46, A: Lys50, A: Arg122, A: Asn127, A: Arg133, A: Ser172, A: Val173, A: Gly174, A: Gly175, A: Gln176, A: Ile177, A: Ser178, A: Asp180, C: Pro165, Asp166, C: Gln168) for the saquinavir-2i54 complex. In the grazoprevir-2i54 complex, it is found that twelve hydrogen bonds (A: Arg19, A: Lys50, A: Asn70, A: Arg122, A: Ser172, A: Val 173, A: Gly175, A: Gln176, A: Lys188, A: Gly212, A: Gly213, A: Asn214), out of these amino acids Gly212 involved 81% to formed hydrogen bond with grazoprevir, seven hydrophobic interactions (A: Leu72, A: Arg122, A: Met125, A: Val173, A: Phe182, A: Lys188, A: Tyr216), three ionic bonds (A: Asp12, A: Arg19, A: Lys50) and twenty-four water bridges (A: Asp12, A: Arg19, A: Gly45, A: Ser46, A: Asp47, A: Lys50, A: Glu69, A: Asn70, A: Arg122, A: Asn123, A: Arg133, A: Arg140, A: Tyr171, A: Ser172, A: Val173, A: Gly174, A: Gly175, A: Gln176, A: Asp180, A: Lys188, A: Lys208, A: Gly212, A: Gly213, A: Asn214). Table 3 Thus, based on these interactions, grazoprevir-2i54 and saquinavir-2i54 complexes demonstrated outstanding stability and interactions throughout the simulation (Figure 3C-D).

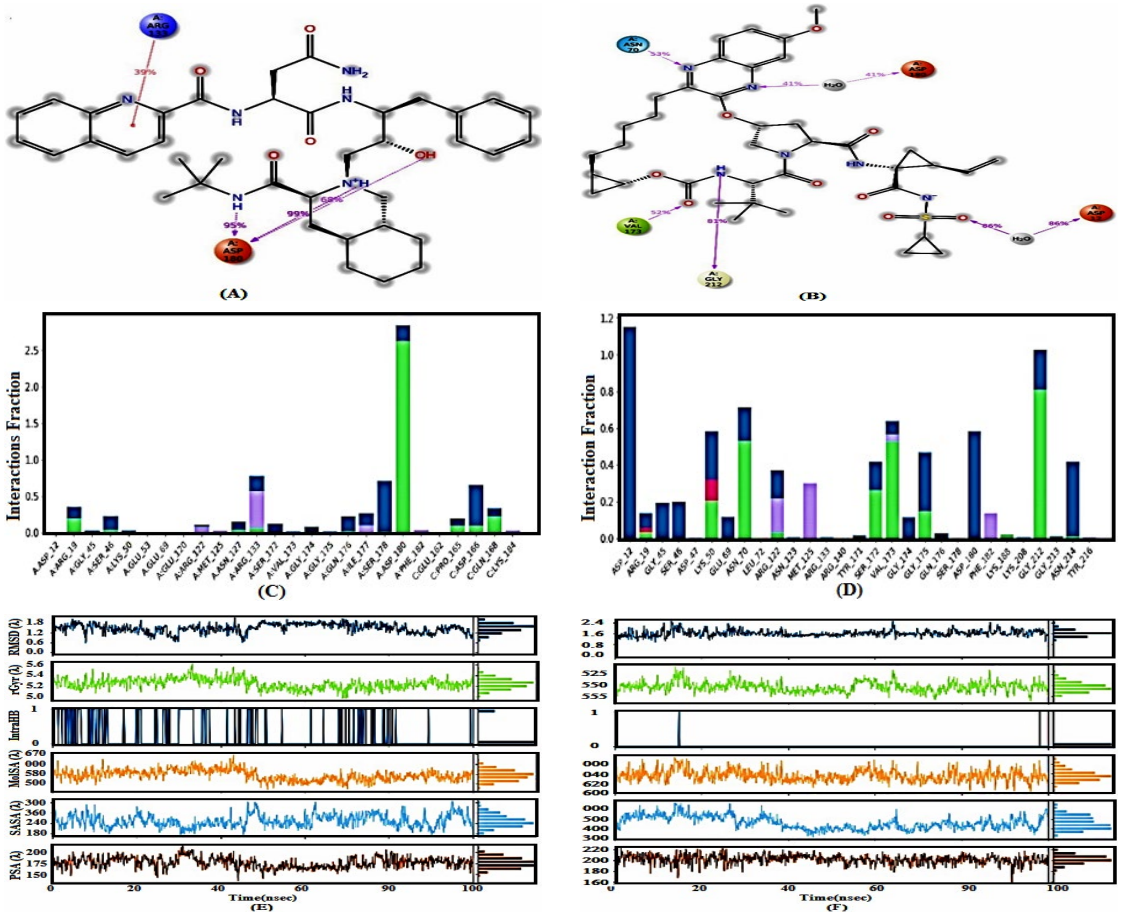

Fig. 3. (A-B) 2D-structure of Saquinavir and Grazoprevir interaction with 2i54 receptor. (C-D) In histogram displayed the bond interaction with amino acids during 100ns molecular dynamics simulation. (E-F) Ligand contact properties viz. RMSD (Blue Line), Radius of Gyration (Green Line), Molecular Surface Area (Orange line), Solvent Accessible Surface Area (Cyan blue line), and Polar Surface Area (Brown line)

DISCUSSION

Leishmania is a vector-borne, obligate intracellular, protozoan parasite causing cutaneous, mucocutaneous, and visceral disease, roots for health problems in many countries.[33] Leishmaniasis is a neglected tropical disease infecting 90 countries including Asia, Africa, the Middle East, and Central and South America throughout the world. The current estimations of CL occurrence range from 700,000 to 1.2 million cases per year.[34]

For the treatment of leishmaniasis, some drugs are used including Amphotericin B, Fluconazole, Ketoconazole, Miltefosin etc. which cause severe adverse effects for long time treatment.[20] The need for vaccines against leishmaniasis is most urgent. Drug repurposing is a unique strategy for neglected diseases may shorten the time and expenses, fewer clinical trial phases are needed to reach the drugs in the market. It also encourages the creation of new mechanisms of action for both new and existing medications, allowing the project to move quickly toward disease-oriented development.[35]

In this study, we targeted PMM [PDB ID: 2i54] from leishmania using drug repurposing approaches to narrow down the most efficacious drugs for potential treatment. The results of the entire article stressed the potential inhibitory role of Saquinavir and Grazoprevir based on virtual drug screening, molecular docking, and MD simulation[36] which demonstrated more stability and well fitted than miltefosine in the active site of the receptor. The docking results were validated by performing an MD simulation study. During the MD simulation, the RMSD values 1.582-4.935 and 1.935-5.655 estimated for Saquinavir and Grazoprevir complexes. According to our study, both compounds held up their stability throughout the 100ns simulation and showed efficiency as potent drug candidates against cutaneous leishmaniasis. This study will help to perform *In vitro* and *In vivo* studies of Saquinavir and Grazoprevir for CL.

CONCLUSION

A drug repurposing study was carried out to find novel drugs against PMM (2i54). Thus, 8500 approved drugs from the Zinc database were screened initially using a virtual screening tool, and selected the top 46 drugs based on a high binding score. The molecular docking simulation of the top 46 drugs were carried out by using the Glide module of Schrodinger software which hypothesized that grazoprevir and saquinavir could act as promising PMM inhibitors. The results showed that the threshold binding affinity of saquinavir and grazoprevir are -10.144 and -10.131 kcal/mole for PMM respectively. Further, we performed MD simulation of saquinavir-2i54 and grazoprevir-2i54 at 100ns. In the grazoprevir-2i54 complex, the RMSD values of ligand 1.075-3.663 Å with the RMSF value of protein 0.498-3.835Å as well as the RMSD value of ligand in saquinavir-2i54 was noted that 0.979-4.937Å with RMSF value 0.690-5.526 Å of the protein. Both complexes exhibited good stability in the binding pocket against the target receptor. Our work could provide new possibilities for the treatment of CL.

ACKNOWLEDGMENT

The authors gratefully acknowledge the R&D wing of Integral University, Lucknow, for providing communication number IU/R&D/2021-MCN0001328.

REFERENCES

1. Matadamas-Martínez, F.; Hernández-Campos, A.; Téllez-Valencia, A.; Vázquez-Raygoza A.; Comparán-Alarcón S.; Yépez-Mulia, L.; Castillo, R. *Mole.*, **2019**, *24*, 3216.
2. Aoki J. I.; Muxel, S. M.; Cristina, J.; Fernandes, R.; Floeter-Winter, L. M. Scientific Reports **2018**, 75867
3. Murray, H. W.; Berman, J. D.; Davies, C. R.; Saravia, N.G. *Lancet*., **2005,** *366*(9496), 1561-77.
4. Saker L.; Lee, K.; Cannito, B.; Gilmore, A.; Campbell-Lendrum, D. Globalization and infectious diseases: a review of the linkages. UNICEF/UNDP/World Bank/WHO Special Programme for Research and Training in Tropical Diseases. TDR/STR/SEB/ST/04.2. Geneva, World Health Organization., **2004**.
5. WHO report **2021**, https://www.who.int/.../data/themes/topics/topic-details/GHO/leishmaniasis.
6. Aronov, A. M.; Suresh, S.; Buckner, F. S.; Van Voorhis, W. C.; Verlinde, C. L.; Opperdoes, F. R. *Proc. Natl. Acad. Sci. U.S.A.*, **1999**, *96*, 4273–4278.

7. Chowdhury, S. F.; Villamor, V. B.; Guerrero, R. H.; Leal, I.; Brun, R.; Croft, S. L.; Goodman, J. M.; Maes. L.; Ruiz-Perez, L. M.; Pacanowska, D. G.; Gilbert, I. H. *J Med. Chem.*, **1999**, *42*(21), 4300-4312.
8. Verlinde, C. L. M. J.; Hannaert, V.; Blonski, C.; Willson, M.; Perie, J. J.; Fothergill-Gilmore, L.A.; Opperdoes, F.R.; Gelb, M.H.; Hol, W.G.J.; Michels, P.A.M. *Drug Resist. Updat.*, **2001**, *4*, 50–65.
9. Olin-Sandoval, V.; Moreno-Sanchez, R.; and Saavedra, E. *Curr. Drug Targets.*, **2010**, *11*, 1614–1630.
10. Descoteaux, A.; Luo, Y.; Turco, S. J.; Beverley, S. M. *Scien.*, **1995**, *269*, 1869–1872.
11. Descoteaux, A.; Turco, S. *J. Biochim. Biophys. Acta.*, **1999**, *1455*, 341–352.
12. Podinovskaia, M.; Descoteaux, A. *Future Microbiol.*, **2015**, *10*, 111–129.
13. Lamotte, S.; Späth, G. F.; Rachidi, N.; Prina, E. The enemy within: targeting host-parasite interaction for antileishmanial drug discovery. *PLoSNegl. Trop. Dis.*, **2017**, *11*, e0005480.
14. Pomel, S.; Loiseau, P. M.; Molecular Routes to Drug Discoveries, Weinheim: Wiley-VCH Verlag GmbH and Co. KGaA, **2013**, 315–334.
15. Mao, W.; Daligaux, P.; Lazar, Noureddine.; Ha-Duong, T.; Cavé C.; Tilburg, H.; Loiseau, P. M.; Pomel, S. *Scientific repor.*, **2017**, *7*(1), 751.
16. Varki, A. *Natur.*, **2007**, *446*, 1023–1029
17. Colley, K. J.; Varki, A.; Kinoshita, T. "Chapter 4: Essentials in Glycobiology, 3rd Edn., New York, NY: Cold Spring Harbor Laboratory Press, **2017**, 41–49.
18. Pomel, S.; Rodrigo, J.; Hendra, F.; Cavé, C.; Loiseau, P. M. *Parasite.*, **2012**, *19*, 63–70.
19. Frézard, F.; Demicheli, C.; Da Silva, S. M.; Azevedo, E. G.; Ribeiro, R. R.; Nano- and Microscale Drug Delivery Systems, Design and Fabrication, 14th April, **2017.**
20. Luiz, F.; Oliveiraa, Armando O.; Schubacha, M.; Martins M.; Passos, S. L.; Oliveiraa R. V.; Marzochi, M.C.; Andrade, C.A. *Acta Tropica.*, **2011**, *118*, 87–96.
21. Weisman, J.L.; Liou, A.P.; Shelat, A.A.; Cohen, F.E.; Guy, R.K.; DeRis, J.L., *Chem. Biol. Drug. Des.*, **2006**, *67*, 409–416.
22. Chong, C.R.; Jr Sullivan, D. *J. Natu.*, **2007**, *448*, 645–646.
23. Guo, D.; Ji, X.; Luo, J.; Fisher, D. B.; Bolatto, A.; Drory, N.; Tyurenkov, I. N.; Ozerov, A. A.; Kurkin, D. V.; Chen, M. *J. of Phys.: Conf. Ser.*, **2021**, *1893*(1), 012015.
24. Kedzierski, L.; Malby, R. L.; Smith, B.J.; Perugini, M.A.; Hodder, A.N.; Ilg, T.; Colman, P.M.; Handman, E. *J Mol. Biol.*, **2006**, *363*, 215-22.
25. Rai, D.K.; Rieder, E. *Int. J. Mol. Sci.*, **2012**, *13*, 8998-9013.
26. Deshpande R. R.; Tiwari A.P.; Nyayanit, N.; Modak, M. *Eur J Pharmacol.*, **2020**, *886,* 173-430.
27. Irwin, J.; Shoichet, B. *J. Chem. Inf. Model.*, **2005**, *45*, 177–182.
28. Trott, O.; Olson, A. J.; *J. Comput. Chem.*, **2010**, *31*, 455–461.
29. Saddala, M. S.; Kiran P. Adi, J.; Rani, U. A.; *J. Res. and Dev.*, **2016**, *4*(2), 0145
30. Guan, B.; Zhang, C.; Zhao, Y. *Mole.*, **2017**, *22*(12), 2233.
31. Singh, S.; Florez, H. F1000 *Res.*, **2020**, *9*, 502.
32. Ansari, W. A.; Ahamad, T.; Khan, M. A.; Khan, Z. A.; Khan, M. F. *Letters in Drug Design & Discov.*, **2022**, *19*(8), 741-756.
33. Sarah M.; Katherine, F.; Sara, S.; Henao-Martínez, A. F.; Sabrina, N.; Ramanan, José A. S. *Curr. Trop. I Med. Rep.*, **2021**, *8*, 121–132.
34. WHO. Leishmaniasis, **2022** [Available from: https://www.who.int/news-room/fact-sheets/detail/leishmaniasis].
35. Sudeep, P.; Francesco, I.; Eyers P. A.; Jane, E. K.; Hopper, S.; Andrew, W.; Andrew, D.; Tim, G.; Joanna, L.; Christine, M. N.; Alan, N.; Philippe, S.; Cavalla, D.; Munir, P. *Nat Rev. Drug Discov.*, **2019**, *18*(1), 41-58.
36. Khana, A.; Alib, S. S.; Khan, M. T.; Saleem, S.; Ali, A.; Suleman, M.; Babar, Z.; Shafiq, A.; Khane, M.; Dong-Qing W.; *J. Biomole. Stru. & Dynam.*, **2021**, *39*(13), 4659-4670.